Road Surface Recognition at mm-Wavelengths Using a Polarimetric Radar

Citation for the original published paper (version of record):
Vassilev, V. (2021)
Road Surface Recognition at mm-Wavelengths Using a Polarimetric Radar
IEEE Transactions on Intelligent Transportation Systems, In Press
http://dx.doi.org/10.1109/TITS.2021.3066312

(article starts on next page)

Road surface recognition at mm-wavelengths using a polarimetric radar

Vessen Vassilev

***Abstract*—We demonstrate detection of ice formations on a road surface using a polarimetric radar operating at 87.5-92.5 GHz. The radar measures the scattering parameters of the surface at horizontal and vertical polarizations and their cross-polarization components. We demonstrate detection of ice for radar beam directed at up to 45^0 angle of incidence with respect to the surface which allows for road surface characterization in front of a vehicle.**

The method used is based on a statistical approach where the 2-port scattering parameters are measured multiple times and used to calculate an average scatter coherence matrix representing the surface. The coherence matrix is then decomposed to eigenvalues/vectors, which are used to estimate polarimetric attributes such as target entropy(degree of randomness) and polarimetric pedestal (degree of depolarization).

Through measurements of dry, ice-covered and wet road surfaces, we show that both entropy and depolarization are increased with respect to dry surface when a thin ice layer is formed, while their value decrease for the case of wet surface. It is also shown that these polarimetric attributes are not sensitive to surface roughness in dry conditions, minimizing the probability of false alarm due to road surface wear.

***Index Terms*—Radar polarimetry, Ice, road surface identification, target entropy**

I. Introduction

Thin formations of ice on road surfaces contribute to traffic accidents in winter and cause many casualties all over the world. A sensor capable of detecting ice in front of a moving car can deliver warning to the driver or the control system of the vehicle. Mm-wavelengths are attractive for traffic safety related applications due to their short wavelengths, which allow building compact antennas in combination with availability of technology and frequency spectrum. Mm-wave radars are already commonly used in modern cars to analyse the traffic surrounding and can potentially be adapted to distinguish between dry/icy or wet road surfaces.

Previous studies to detect ice formations on road surfaces include a 61 GHz bistatic polarimetric radar sensor capable of distinguishing various types of surfaces under a moving vehicle as presented in [1], and a 24 GHz monostatic sensor [2] both measuring backscattering coefficients for vertical, horizontal and cross polarizations.

A method of surface classification is presented in [3] where a car radar at 20-24 GHz is used to collect and analyze polarimetric data from various surfaces.The data is analyzed using Stokes parameters to extract information about the surface properties.

V. Vassilev is with the Department of Microtechnology and Nano Science at Chalmers University of Technology

Manuscript received October 2020; revised January, 2021.

However, due to the random nature of the distributed target a single measurement is not sufficient to extract reliable information about its surface properties. Therefore, a statistical approach has to be adopted. In this work we use polarimetric attributes such as target entropy (TE), which is a measure of target dissorder and polarimetric pedestal (PP), which is a measure of the degree of depolarization generated by the target, to analyse the surface. After performing a number of monostatic measurements in W-band (75-110 GHz), the polarimetric attributes are derived from the eigenvalues of the averaged coherence/covariance matrix. By comparing TE and PP for dry, wet and ice-covered surfaces, this work shows that these attributes are sensitive to the surface properties .

This manuscript is organised as follows. Section II presents the method of calculating the polarimetric attribute. The measurement setup and its calibration are discussed in section III. The measurement section IV starts by presenting characterization of an asphalt surface for 3 different conditions: ice-covered, dry and wet for the frequency band 87.5-92.5 GHz. Measurements of a second sample of a road surface with a higher roughness are presented for 2 cases: dry and ice-covered. Subsection IV-C compares both surfaces in dry condition and shows that the polarimetric attributes are not sensitive to roughness. At the end of section IV results are presented for the full frequency coverage of the radar 75-110 GHz to show that high range resolution does not contribute to better distinguish ice-covered from dry and wet surfaces when polarimetric attributes are used. At the end of the measurement section the polarimetric attributes are presented as a function of the number of measurements to confirm that convergence can be reached with a reasonable number of measurements.

II. Method

Even though asphalt is a surface with uniform properties, it represents a random distributed target and can exhibit large variations from one illumination area to another. A statistical approach is needed in order to extract useful information about the properties of the surface. Target entropy (TE) [4] and polarimetric pedestal (PP) [5] are two polarimetric attributes, which are calculated from the eigenvalues of the coherence matrix.

The relation between the 2-port scattering matrix and the corresponding matrix in the case of radar backscattering is given by:

$$\begin{bmatrix} S_{11} & S_{12} \\ S_{21} & S_{22} \end{bmatrix} = \begin{bmatrix} S_{VV} & S_{VH} \\ S_{HV} & S_{HH} \end{bmatrix} \quad (1)$$

The reciprocity theorem of backscattering states that $S_{HV} = S_{VH}$ [6] and the coherence matrix as defined in [4] is reduced

to *3x3* elements. The coherence matrix can be represented as the product of the coherence vector k with its transposed complex conjugate:

$$T = kk^{\dagger} \tag{2}$$

where the coherence vector k is given by:

$$k = \begin{bmatrix} S_{HH} + S_{VV} \\ S_{HH} - S_{VV} \\ 2S_{HV} \end{bmatrix} \tag{3}$$

To calculate the eigenvalues and eigenvectors of the coherence matrix a minimum of 3 measurements are needed. For a set of N number of measurements, the measurement matrix M consists of N columns of the measured coherence vector in the presence of noise.

$$M = \begin{bmatrix} | & | & .. & | \\ k^1 & k^2 & .. & k^N \\ | & | & .. & | \end{bmatrix} \tag{4}$$

An estimate of the coherence matrix $\hat{T}$ is obtained by multiplying the measurement M matrix with its transposed complex conjugate and dividing by the number of measurements.

$$\hat{T} = \frac{MM^{\dagger}}{N} \tag{5}$$

The coherence matrix is then decomposed, and the 3 eigenvalues ($\lambda 1$, $\lambda 2$ and $\lambda 3$) are extracted. The physical interpretation of the eigenvalues can be found in [7] and suggests that $\lambda 3$ depends on the cross polarization return, which associates this eigenvalue with diffuse scattering. Scattering resulting from odd and even number of reflections is represented by $\lambda 1$ and $\lambda 2$, respectively. Entropy is a measure of the randomness of the scattering process and has a value of 0 for a single non-random target and 1 for a highly random distributed target. The entropy is given by [4]:

$$H = -\sum_{i=1}^{3} Pi.\log_3(Pi) \tag{6}$$

where Pi has a meaning of probability and represents the relative importance of the corresponding eigenvalue with respect to the total scattered power. Pi is given by:

$$Pi = \frac{\lambda i}{\lambda 1 + \lambda 1 + \lambda 3} \tag{7}$$

The PP, which is a measure of the degree of depolarization generated by the target is given by [5]:

$$P_H = \frac{min(\lambda 1, \lambda 2, \lambda 3)}{max(\lambda 1, \lambda 2, \lambda 3)} \tag{8}$$

Identical values of TE and PP are obtained if the covariance matrix [7] is used instead of the coherence. In the case of the covariance matrix the elements of the *k*-vector in eq. 3 are replaced by S_{VV}, S_{HV} and S_{HH}.

III. Measurement setup

The measurement setup is shown in Fig. 1. The target response in the time domain is derived from 2-port complex scattering parameters measured in the frequency domain. The measurement is performed at discrete number of frequency points by a vector network analyzer (VNA) [8] using a continuous waveform. To reach mm-wave frequencies, the VNA is extended to the W-band 75-110 GHz using external frequency extenders. To separate the polarizations the frequency extenders are connected to an orthomode transducer (OMT), which is fed by a duo-pol horn antenna equipped with a lens. The isolation between the ports of the OMT is 28 dB. The S11 and S22 scattering parameters correspond to V-V and H-H reflection coefficients, while S12 and S21 are measures of the cross-polarization component (V transmitted-H received and vice versa). The measured S-parameters in the frequency domain are windowed using a Hanning window and transformed to the time domain by an inverse Fourier transform. The scattering parameters are then used to calculate the coherence matrix as described in the previous section.

To calibrate the VNA, the horn is extracted and replaced by a circular- to-rectangular waveguide transition, which is connected to the circular waveguide port of the OMT and aligned with one of the polarizations. The VV-port of the VNA is then calibrated using rectangular waveguide standards. The waveguide transition is then rotated 90^0 and the HH-port is calibrated the same way. For the THRU measurement the OMT was extracted and both frequency extenders were connected together. This introduces a phase error for the S21 and S12 parameters, which is compensated by additional measurement of a surface at 0 angle of incidence. The time domain peaks of S11 and S22 are then aligned with S21 and S12 by adding an additional linear phase component to the frequency domain points of the S21 and S12 vectors. As shown in Fig. 1, the measurement ports of the VNA, the OMT and the horn antenna are mounted on a frame allowing to change the angle of incidence, while keeping the distance to the target the same.

The horn antenna is integrated with a teflon lens, which focuses the beam at a distance of 50 cm, with a beam diameter of 4 cm.

IV. Measurements

Two samples of surfaces were characterized: asphalt 1 with rms surface roughness σ=0.65 mm, and asphalt 2 with σ=1.3 mm. The surfaces were measured in dry and wet conditions and after forming a thin ice layer. Thin ice layers were formed by pre-cooling the surface with liquid nitrogen and then spreading water. Asphalt 1 is also characterised in wet condition. For each type of surface a number of measurements are performed by manually moving the sample at a different location with respect to the radar beam. As the sample is rough and not perfectly planar there is a variation in the surface orientation with respect to the beam, which introduces additional variations in the measured scattering parameters between the measured positions. The measurements are performed over the entire W-band 75-110 GHz corresponding to range resolution 6.5mm considering windowing. To show that high range

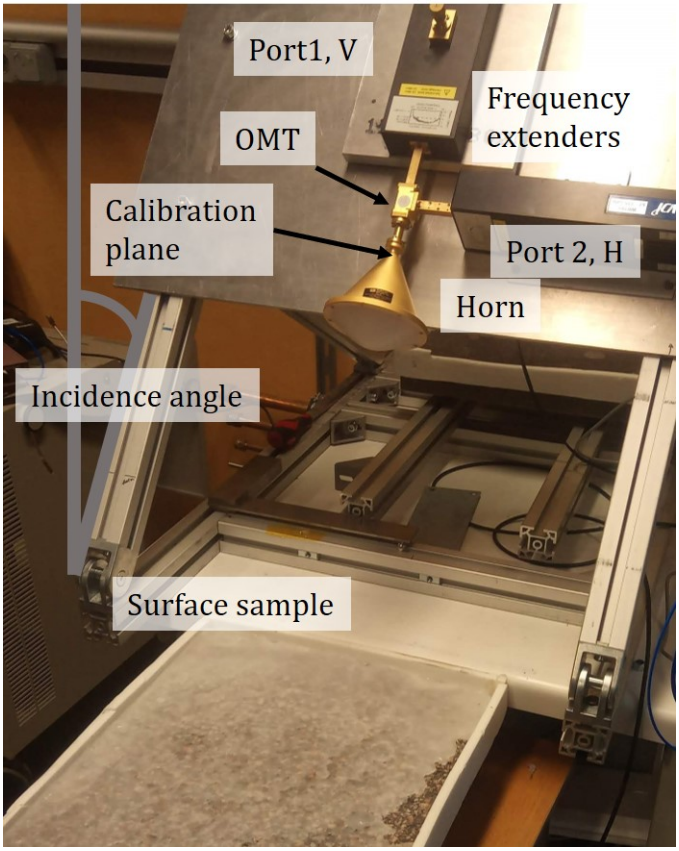

Fig. 1: Measurement setup.

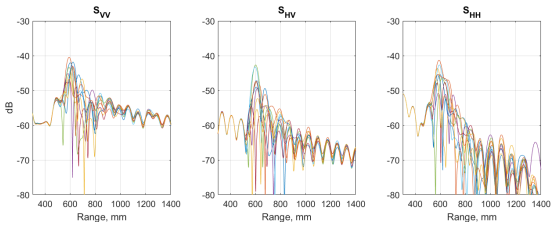

(a) Surface covered with ice.

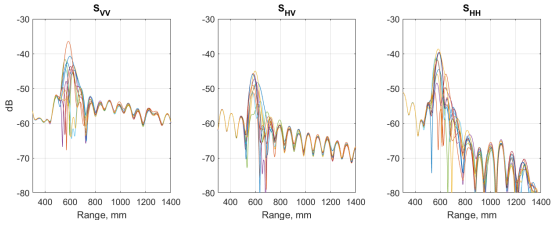

(b) Surface in dry condition.

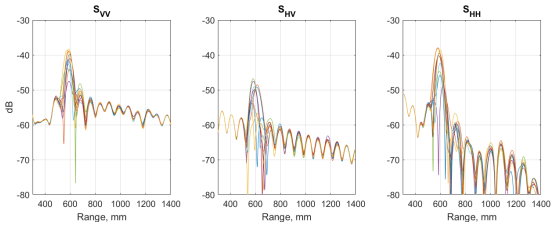

(c) Surface in wet condition.

Fig. 3: Magnitude of the measured scattering parameters transformed in the time domain for surface 1 in icy, dry and wet condition.

resolution is not required when polarimetric attributes are used for the detection of ice, results with maximum range resolution are compared with results for reduced resolution (frequency coverage of 87.5-92.5 GHz, corresponding to range resolution 45 mm considering windowing).

Fig. 2: The Asphalt surfaces measured: dry , wet, and covered with ice. The dry surface has a roughness of σ=0.65 mm. The pictures do not share the same scale.

A. *Polarimetric attributes for dry, ice covered and wet surface*

The measured S-parameters in the frequency domain are windowed and transformed to the time domain. Fig. 3 shows 10 measurements at 10 different positions of the first asphalt surfaces for 3 cases: covered with ice, dry and wet where the frequency domain measurement is limited to 161 frequency points covering the range 87.5-92.5 GHz, corresponding to a range resolution of 45 mm (considering windowing) and unambiguous range of 4829 mm. With IF bandwidth of the instrument set to 1 kHz one sweep is completed in 148 ms considering it takes about 35 us for the instrument to switch frequency. The same measurement performed with 10 kHz of IF bandwidth takes 19 ms.

As observed from the figure there is a large spread of the magnitude of the measured scattering parameters due to the inherent randomness of the distributed target in addition to variations in its orientation between the measurements. Since the measurements are from different parts of the surface, as in the case of a sensor mounted on a moving vehicle, the measured scattering parameters will vary randomly as the illuminated spot moves along the surface.

Based on the measured scattering parameters from Fig. 3 at 10 different positions on the target the coherence matrix $\tilde{T}$ is calculated according to eq. 5 and its eigenvalues are shown in Fig. 4.

After the matrix decomposition the TE and PP are calculated according to eq. 6 and eq. 8 for surface 1 when dry, wet and ice-covered. The result is presented in Fig. 5 as a function of the range.

One interesting observation from Fig. 5 is that the range of visibility (where entropy is higher than 0) of the surface is extended after the surface is covered with ice. This can be explained by the fact that the ice enhances higher order reflections within the target, which contributes to higher entropy. So at closer ranges first order reflections dominate and the surfaces are hardly distinguishable as the values of TE and

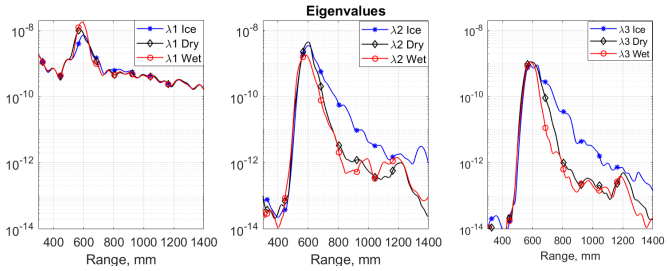

Fig. 4: Eigenvavues for ice-covered, dry and wet surface 1.

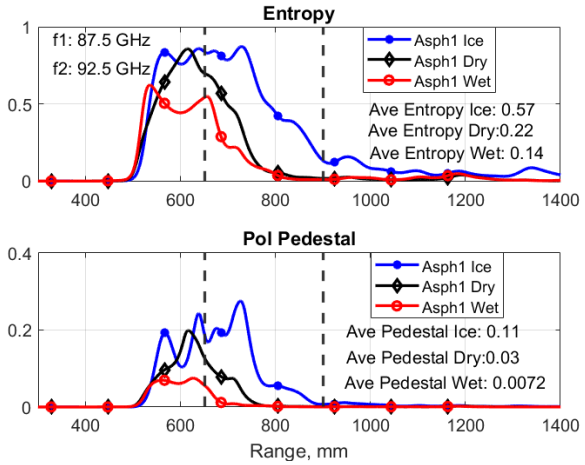

Fig. 5: Calculated TE and PP of surface 1 with roughness σ =0.65 mm for angle of incidence 45^0 when dry, wet and ice-covered. The averaged values are given for the range marked with dashed lines.

PP are similar. For longer ranges (650 to 900 mm) second and higher order reflections dominate, which effectively makes the ice-covered surface look longer compared to the dry surface. This extension of the range where entropy is different is the range where the effect of the ice layer is most visible. This "sweet spot" of range span between 650 to 900 mm is denoted by a dashed line in Fig. 5 and the average values of entropy and polarimetric pedestal are calculated and shown in the figure.

If the asphalt is fully covered by water the surface is specular producing no backscatter. However, for the case of wet asphalt, also shown in Fig. 2, the cavities of the surface are only partly filled with water allowing for backscatter reflection due to the remaining roughness of the surface. The wet surface can be viewed as partially covered by "mirror areas" representing the water filled areas resulting in a more "ordered target" producing lower values for both entropy and depolarization. The difference between the averaged values of both entropy and polarimetric pedestal is sufficient and can be used to distinguish a thin ice layer (in this case of the order of 2-3 mm) from a dry or wet surface.

Table I shows the TE and PP for 36^0 and 45^0 angles of incidence, indicating identical values of TE and PP for icy surface and similar values for dry and wet surface, with TE and PP slightly higher for the 36^0 angle of incidence. This shows that the polarimetric attributes are not very sensitive to the angle of incidence and can tolerate variations of the angle during measurements.

TABLE I: Target Entropy and Polarimetric Pedestal.

Incidence Angle	TE Ice	TE Dry	TE Wet	PP Ice	PP Dry	PP Wet
36^0	0.57	0.38	0.16	0.11	0.065	0.0095
45^0	0.57	0.22	0.14	0.11	0.03	0.0072

B. Surface 2 with and without ice

To verify the measurements presented above a second surface was characterized, from the same material but of higher roughness, σ =1.3 mm. The calculated TE and PP for dry and icy surface, shown in Fig. 6, show similar values as for surface 1 in Fig. 5.

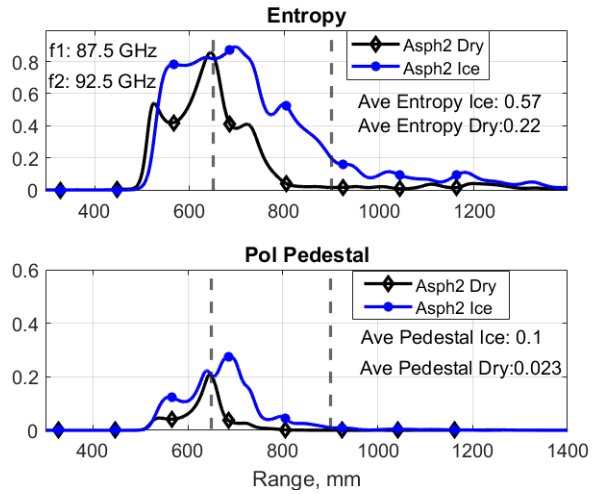

Fig. 6: Calculated TE and PP for dry and ice-covered surface 2 with roughness σ =1.3 mm for angle of incidence 45^0. The averaged values are given for the range marked with dashed lines.

C. Surface 1 and 2 in dry condition

In real traffic conditions the surface roughness may vary rapidly from section to section depending on the surface wear. It is therefore of interest to see if surfaces with different, but comparable roughness give the same values of TE and PP. As seen in Fig. 5 and 6 the averaged values of TE and PP for surface 1 are similar to the corresponding values of surface 2, suggesting that both TE and PP are not sensitive to surface roughness at least within certain limits.

D. Range resolution

In the sections presented above the measured S-parameters are limited to 87.5-92.5 GHz frequency range, corresponding to 45 mm range resolution. Fig. 7 presents calculated entropy and polarimetric pedestal for the full frequency band available from the measurement setup. The surfaces are as above, but the bandwidth is expanded to 75-110 GHz corresponding to range resolution 6.5mm (considering windowing). Fig. 7 indicates

that the averaged TE and PP values for the full range resolution are similar to the case of reduced range resolution from Fig. 5. One benefit of using polarimetric attributes for road surface characterization is that there is no need for broad frequency coverage of the radar (high range resolution). The polarimetric attributes of icy, dry and wet surfaces can be distinguished with a range resolution as low as 75 mm (3 GHz bandwidth). For even lower range resolution the peaks of TE and PP get smeared in range and the "contrast" between ice, dry and wet surface is reduced.

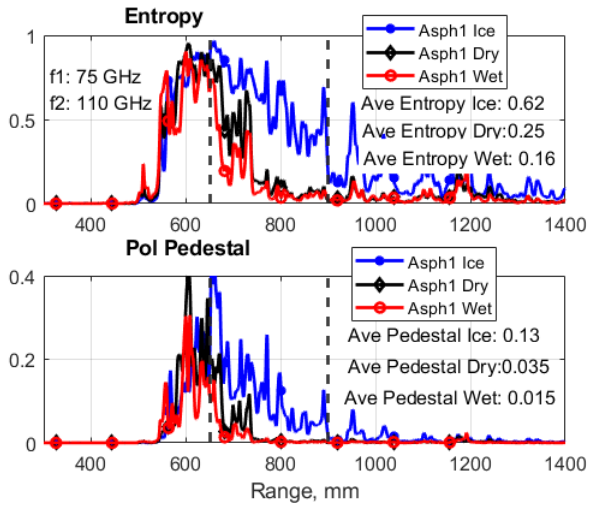

Fig. 7: Calculated TE and PP for surface 1 with maximum range resolution of 6.5 mm (frequency coverage 75-110 GHz). The averaged values are given for the range marked with dashed lines.

E. Convergence of the polarimetric attributes

The rank of the averaged coherence or covariance matrix is 3, so at least 3 measurements are needed in order to decompose the matrix and find the eigenvalues. The noise floor of the radar, the target cross section and degree of randomness determine how many measurements are needed to achieve convergence in the estimated polarimetric attributes. In addition, angle of incidence, surface roughness and dielectric properties are also parameters affecting the convergence. Fig. 8 shows the averaged values of entropy and polarimetric pedestal as a function of the number of measurements (see eq. 4). The averaging values are for range 650-900 mm, also indicated in Fig. 5 to 7.

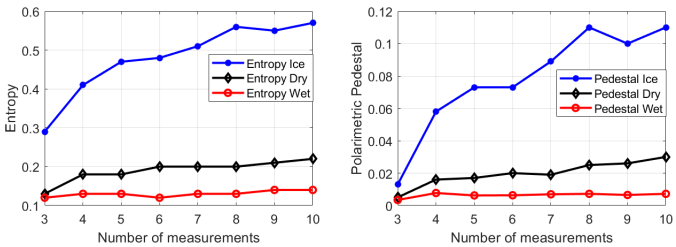

Fig. 8: The averaged TE and PP as a function of the number of measurements for surface 1 at 45^0 angle of incidence.

Fig. 8 shows that the ice-covered surface, which also has higher TE needs more measurements to reach convergence compared to the dry and wet surfaces. In contrast, the wet surface, which is least random converges fastest.

V. Conclusion

This work demonstrates the capability of polarimetric radar measurements at high angle of incidence and the feasibility of using polarimetric attributes to characterize critical properties of surfaces relevant to traffic safety.

Ice-covered surfaces are well distinguished from dry as a result of an increased level of high order reflections within the volume under the surface being illuminated, increasing the values of entropy and polarimetric pedestal. The wet surface on the other hand enhances surface reflection and reduces higher order reflections from the volume below the surface, resulting in decreased values of both TE and PP.

The large difference in the values of TE and PP for dry, icy and wet surfaces demonstrates the capabilities of the polarimetric attributes to distinguish dry from wet and ice-covered surfaces. This opens a possibility to construct a radar that is capable of detecting road surface properties in front of a moving vehicle and can thus warn the driver for areas of low friction before the tyres reach the surface.

The measurement results on typical road surfaces suggest that the range-span of visibility of the target is about 300 mm in the case of entropy, which extends to 400 mm when the surface is covered by a thin layer of ice, and narrows when partially covered with water (see Fig. 5 and 6).

This work suggests that ice can be detected based on the additional second and higher order reflections that occur when ice is formed and not based on measuring its thickness, which would require high range resolution for small thicknesses. Using polarimetric attributes relaxes the requirements on range resolution of the radar dramatically. This work shows that large frequency coverage is not required and demonstrates that 5 GHz of bandwidth is sufficient to distinguish a thin layer of ice from dry and wet surfaces. Both TE and PP are sensitive to the additional reflections that ice introduces and are not sensitive to the roughness of the surface implying a low risk of false alarms resulting from shifting from one surface roughness to another in the absence of ice. In addition it is shown that the polarimetric attributes are not very sensitive to the angle of incidence and can tolerate the variations expected in real traffic conditions.

The measurements presented in the manuscript were performed on a static target. A radar installed on a moving vehicle will produce a frequency offset for the reflected wave. This will result in time varying S-parameters with frequency proportional to the vehicle speed. One way to estimate and compensate the Doppler frequency offset is to consider the phase slope of the samples used in each frequency point. The phase slope will be linearly proportional to the Doppler frequency, fitting a line to the phase of the samples will give an estimate of the frequency offset and the phase of the scattering parameters.

The instrument used in this work [8] is a sort of stepped frequency continuous wave radar. It has advantage of wide

dynamic range, high mean power, possibility of applying different windowing to the data, but most importantly, it is easy to calibrate in polarimetric mode of operation. The drawback is the speed as it takes relatively long time to switch between frequency points (estimated time for switching is 35 us). The speed can be improved if a dedicated radar is designed, instead of using a laboratory instrument.

ACKNOWLEDGMENT

This work is a part of a project entitled "Hardware for next generation millimeter wave automotive radar sensor" financed by Sweden's innovation agency Vinnova within the program "Strategic vehicle research and innovation".

REFERENCES

[1] N. Kees, J. Detlefsen, "Road surface classification by using a polarimetric coherent radar module at millimeter waves", *IEEE MTT-S International Microwave Symposium Digest*, May 1994.
[2] V. Viikari, "Road-Condition Recognition Using 24-GHz Automotive Radar", *IEEE Transactions on Intelligent Transportation Systems, Vol. 10, No. 4*, December 2009.
[3] H. Rudolf, G. Wanielik, A.J. Sieber, "Road condition recognition using microwaves", *Proceedings of Conference on Intelligent Transportation Systems*, Nov. 1997.
[4] S. H. Cloude, "An Entropy Based Classification Scheme for Land Applications of Polarimetric SAR", *IIEEE Transactions on Geoscience and Remote Sensing*, (vol. 35), Jan. 1997.
[5] S.L. Durden, et. al.,"The unpolarized component in polarimetric radar observations of forested areas", *IEEE Transactions on Geoscience and Remote Sensing (Volume: 28 , Issue: 2*, Mar 1990.
[6] Tsang L., et. al., "Theory ofMicrowave Remote Sensing", *Wiley and Sons*, April 1985.
[7] Ulaby, "Microwave radar and radiometric remote sensing", *The University of Michigan Press*, 2014.
[8] Keysight Technologies, N5242A PNA-X Microwave Network Analyzer, 10 MHz to 26.5 GHz.
[9] S. H. Cloude, "Recent Developments in Radar Polarimetry: A Review", *AMPC Asia-Pacific Microwave Conference,*, Aug. 1992.
[10] S. H. Cloude, "A Review of Target Decomposition Theorems in Radar Polarimetry", *IIEEE Transactions on Geoscience and Remote Sensing*, April 1996.

Vessen Vassilev received M.Sc. degree in radio communications from Sofia Technical University, Sofia, Bulgaria, in 1995, and M.Sc. degree in digital communications from Chalmers university of technology, Gothenburg, Sweden, in 1998. In 2003 he received a Ph.D. degree from the department of radio and space science at Chalmers. From 1998 to 2008, he was involved in the development of cryogenic millimeter-wave receivers for applications in radio astronomy and space sciences. Instruments designed by him have been in operation at the Atacama Pathfinder Experiment (APEX) Telescope in Chile and Onsala Space Observatory in Sweden. Since 2008, he is with the microwave electronics laboratory, department of microtechnology and nanoscience at Chalmers. His current research interests include the development of millimeter-wavelength sensors based on monolithic microwave integrated circuit technologies.